

Supplementary Information

Insights into arsenic retention dynamics of Pleistocene aquifer sediments by *in situ* sorption experiments

Harald Neidhardt^{a*}, Lenny H.E. Winkel^{b,c}, Ralf Kaegi^b, Caroline Stengel^b, Pham T.K. Trang^d, Vi M. Lan^d, Pham H. Viet^d, and Michael Berg^b

^aGeoecology, Eberhard Karls University Tübingen, 72070 Tübingen, Germany

^bEawag, Swiss Federal Institute of Aquatic Science and Technology, 8600 Dübendorf, Switzerland

^cInstitute of Biogeochemistry and Pollutant Dynamics, ETH Zurich, Universitaetsstrasse 16, CH-8092 Zurich, Switzerland.

^dResearch Centre for Environmental Technology and Sustainable Development (CETASD), Hanoi University of Science, Vietnam National University, Hanoi, Vietnam.

*harald.neidhardt@uni-tuebingen.de

Table of contents:

Fig. S1. Conceptual model of the investigation area in Van Phuc.

Fig. S2. Location of the experimental wells within the study area.

Fig. S3. XRD spectra of Pleistocene sediment recorded from freeze-dried, unexposed sample material.

Fig. S4. XRD spectra of synthetic Fe(III)-(hydr)oxides used for the coating of cristobalite grains.

Fig. S5. Filtration experiment testing groundwater for the presence of particle-associated As.

Fig. S6. Correlation between the BET surface area and the Fe content of ferrihydrite-coated sand.

Fig. S7. Changes in As sorption and Fe contents of samples exposed to the monitoring wells AMS-15, AMS-1 and AMS-5 wells over different time intervals.

Fig. S8. SEM images of representative sample surfaces before and after *in situ* exposure.

Fig. S9. SEM images of ferrihydrite-coated sand samples, including on-spot EDX spectra of selected regions of interest (green squares).

Fig. S10. SEM images and EDX spectra of goethite-coated sand.

Fig. S11. SEM images and EDX spectra of hematite-coated sand.

Table S1. Summary of field parameters and water chemistry for groundwater from the experimental wells.

Table S2. Summary of initial sample material used for the experiments.

Table S3. Summary of experimental data showing the total Fe and As contents of the samples before and after the in situ experiments.

Table S4. Saturation index (SI) values calculated for relevant Fe mineral phases.

Table S5. Absolute and relative differences between As adsorbed to the Pleistocene sediment after one week and six months.

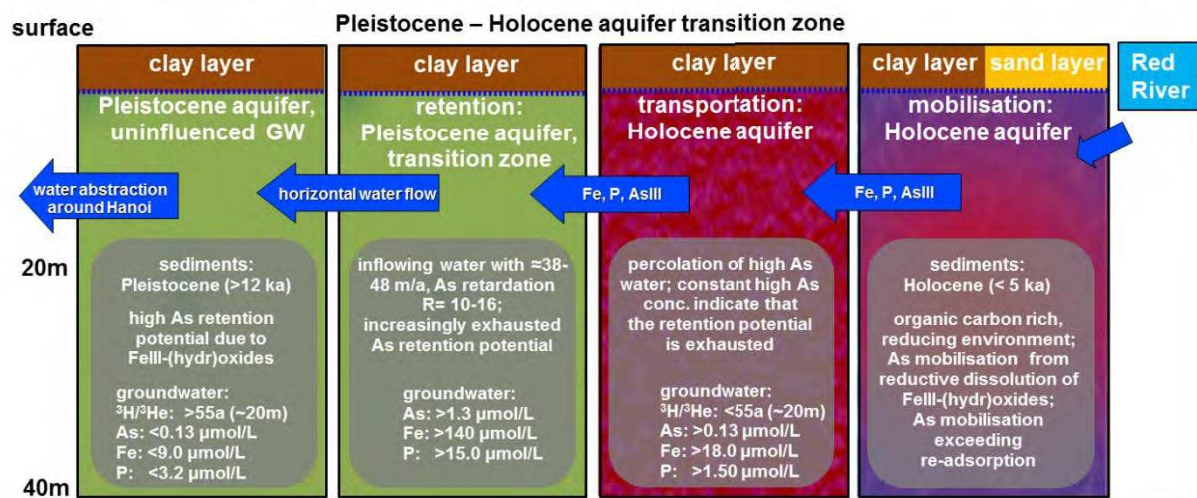
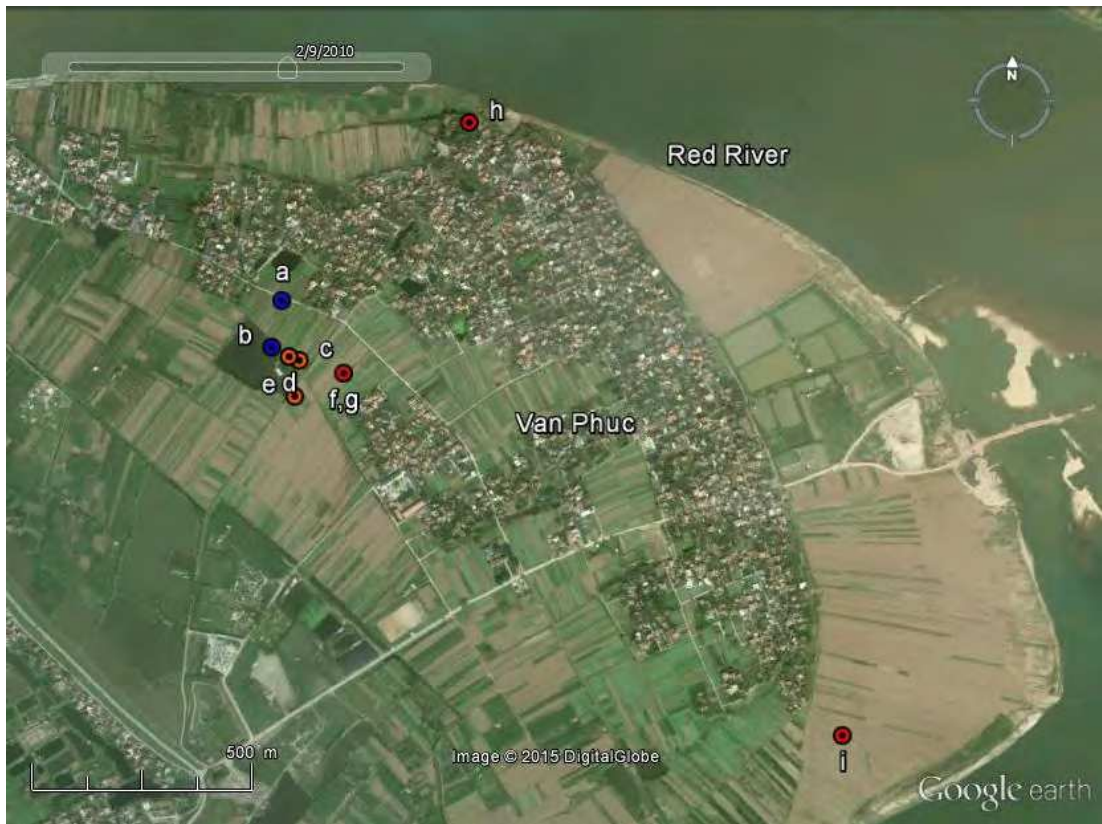


Fig. S1. Conceptual model of the investigation area in Van Phuc. The natural groundwater flow direction has been redirected into north-western direction due to massive groundwater abstraction in the vicinity of Hanoi. As a consequence, high As water horizontally migrates from the Holocene aquifer (where As is being liberated due to the reductive dissolution of As-hosting Fe(hydr)oxides) into the adjacent Pleistocene aquifer. At the transition between both aquifers, As is being retained by Fe mineral-rich Pleistocene aquifer sediments resulting in the build-up of an As legacy (Al Lawati et al. 2012, Eiche 2009, Eiche et al. 2008, van Geen et al. 2013, Weinman et al. 2008).



well ID	screen interval (m bls)	water level* (m bls)	aquifer geology	coordinates		experimental details					
				latitude	longitude	1d	1wk	4wks	6mos	e	
(a) AMS-2	24-25	8.98	P	20°55'22.80"N	105°53'36.96"E				x		d
(b) AMS-4	37-38	nd	P	20°55'19.38"N	105°53'36.17"E		x				a
(c) AMS-11	24-25	7.64	T	20°55'18.42"N	105°53'38.34"E		x		x		a
(d) AMS-32	24-25	nd	T	20°55'18.69"N	105°53'37.53"E		x	x			a
(e) AMS-1	24-25	7.98	T	20°55'15.78"N	105°53'37.98"E		x	x	x	x	a
(f) AMS-5	23-24	8.11	H	20°55'17.47"N	105°53'41.82"E	x	xx	x	x	x	a
(g) VPNS-5	30-31	7.94	H	next to AMS-5				x	x	x	a
(h) AMS-15	27-28	nd	H	20°55'35.84"N	105°53'51.68"E		x	x	x	x	a
(i) AMS-12	24-25	7.95	H	20°54'50.95"N	105°54'20.94"E		x		x	x	a

*water level April 2013

x: six month exposure during rainy season (Apr – Oct); x: six month exposure during dry season (Oct - Apr)

Fig. S2. Location of the experimental wells within the study area. The two inch wells are equipped with one-meter long well screenings (screen intervals provided in the figure above). The wells represented by blue circles draw low As (<0.13 µmol/L) water from sediments of the Pleistocene aquifer (P). The wells represented by orange circles are situated in the transition zone (T) and deliver high As groundwater from Pleistocene sediments. Red circles depict wells that are filtered in young sediments of the Holocene aquifer (H), where groundwater is characterized by high As concentrations (see Table S1 for further details regarding the groundwater chemistry). Experimental details are provided below the figure (a: adsorption experiment, d: desorption experiment). Water levels were determined in April 2013. Previous water level measurements (carried out between October 2012 and April 2013) showed that fluctuations within the water levels of the respective wells remained less than 0.85 m.

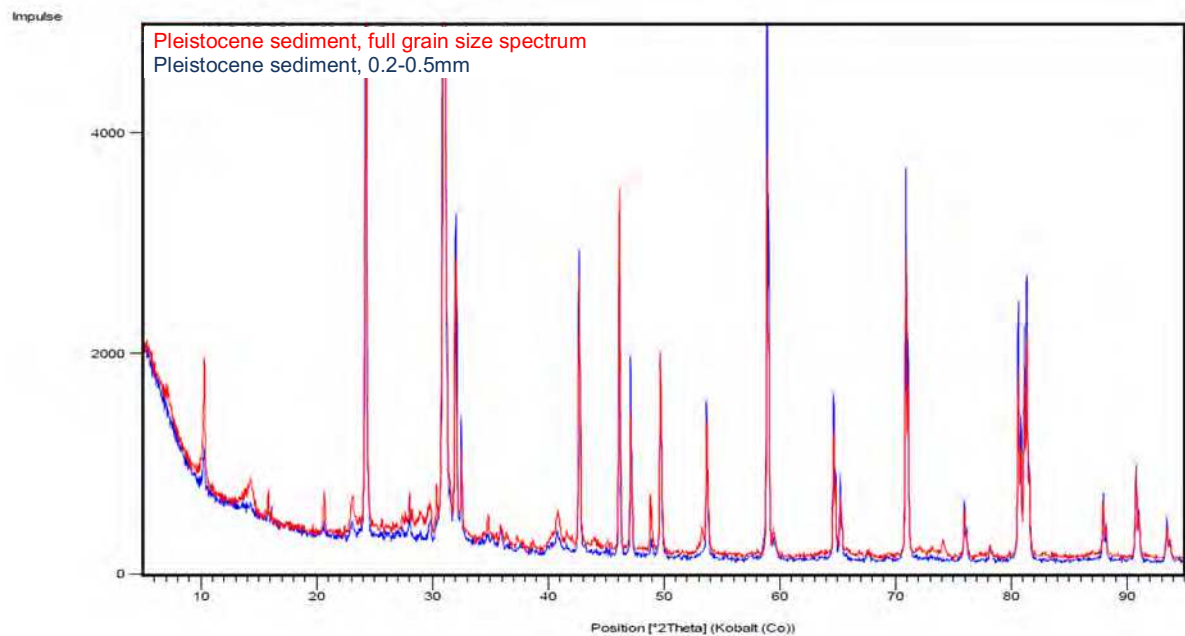


Fig. S3. XRD spectra of Pleistocene sediment recorded from freeze-dried, unexposed sample material. The spectra represent both, unaltered (red spectrum) and sieved (0.2-0.5mm) sample material (blue spectrum). Only a few peaks show a reduced intensity after sieving, while the principal mineral composition was not altered.

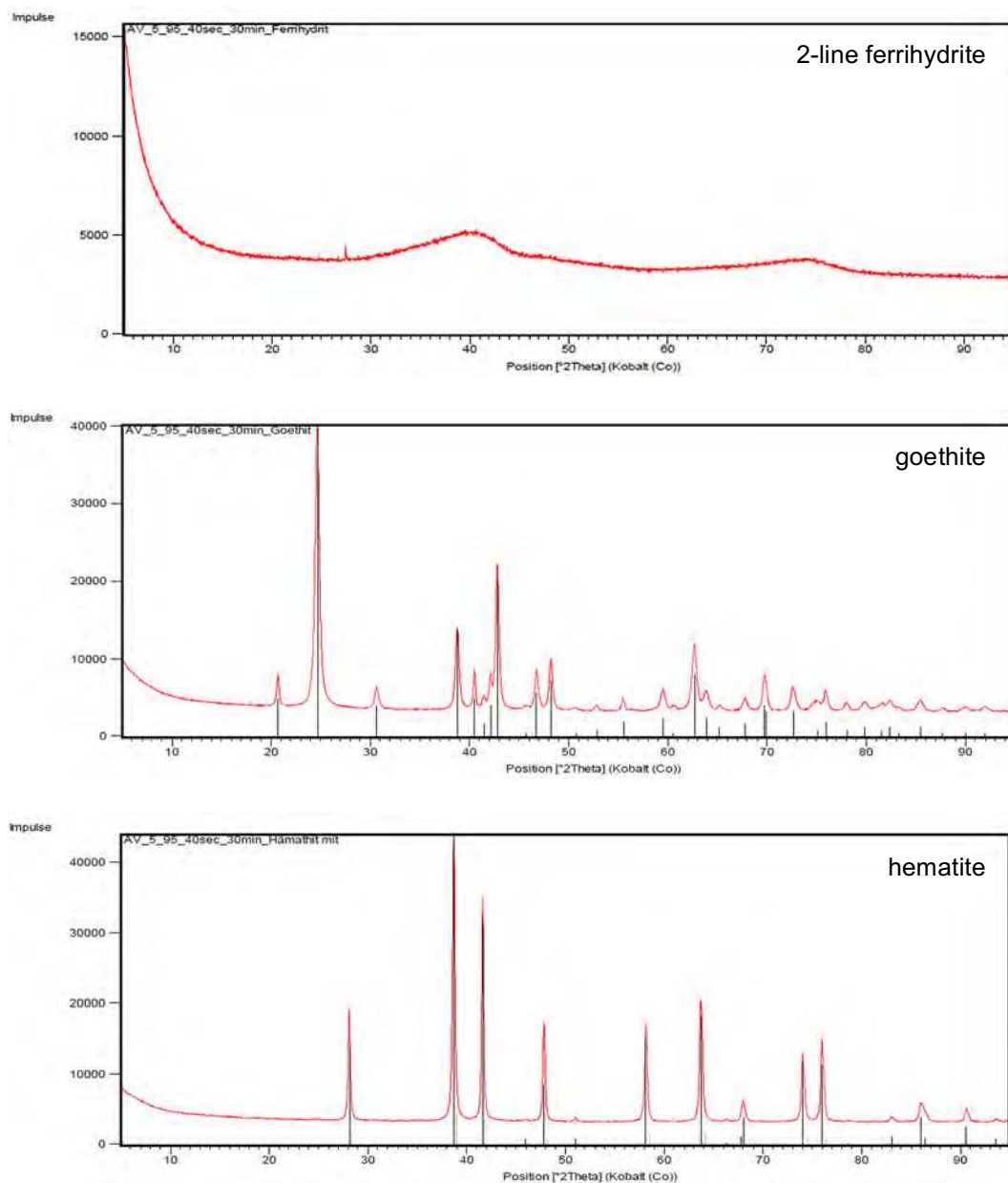


Fig. S4. XRD spectra of synthetic Fe^{III}-(hydr)oxides used for the coating of cristobalite grains. From top to down: two-line ferrihydrite, goethite, and hematite; reference peaks are included for goethite and hematite. The spectra shown confirm the purity of the synthesized minerals.

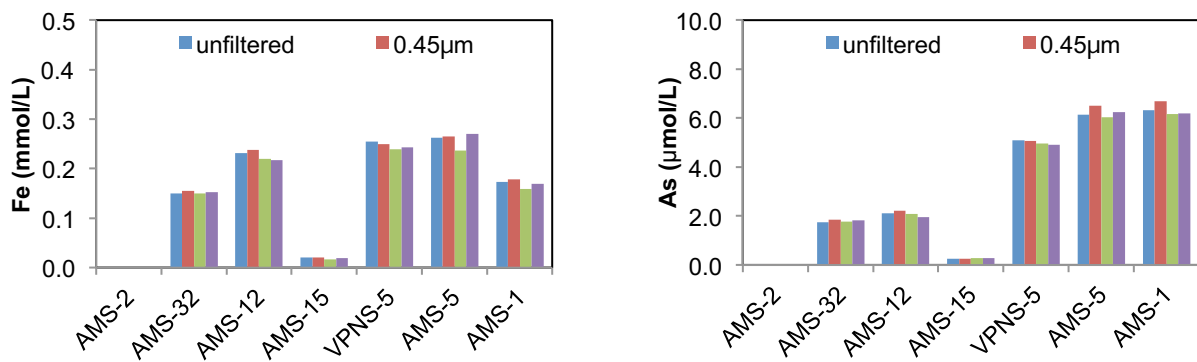


Fig. S5. Filtration experiment testing groundwater for the presence of particle-associated As. Overview of groundwater samples taken in October 2013, which were filtered in parallel through filters of different pore sizes (0.45, 0.2, and 0.1 μm pore size, respectively, cellulose nitrate membrane filters, Whatman). Results show that As and Fe are present as truly dissolved species and not in form of colloids (especially Fe phases), which can serve as a vector for As (Guo et al. 2011).

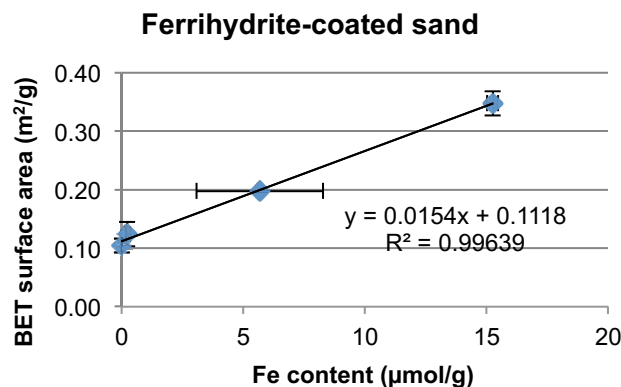


Fig. S6. Correlation between the BET surface area and the Fe content of ferrihydrite-coated samples. From left to right: uncoated cristobalite, long-term exposure (six months) to well AMS-1 and AMS-5, and unexposed initial ferrihydrite-coated cristobalite. Due to the highly positive correlation between the Fe content and the BET surface area, the Fe content was used to extrapolate the remaining surface area of the ferrihydrite samples after *in situ* exposure.

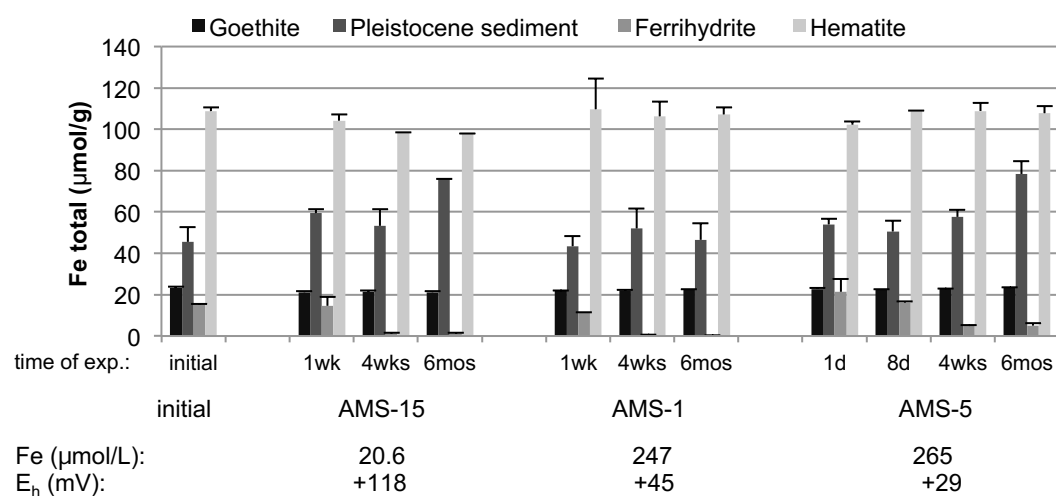
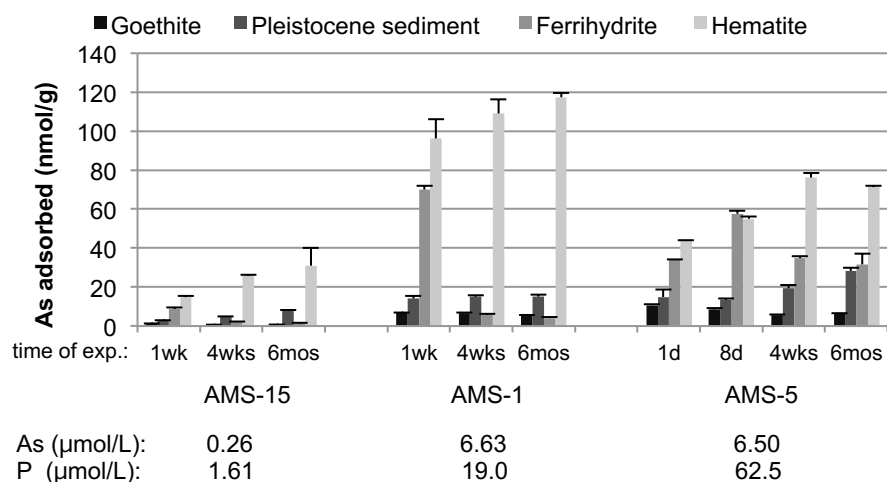


Fig. S7. Changes in As sorption and Fe contents of samples exposed to the monitoring wells AMS-15, AMS-1 and AMS-5 wells over different time intervals.

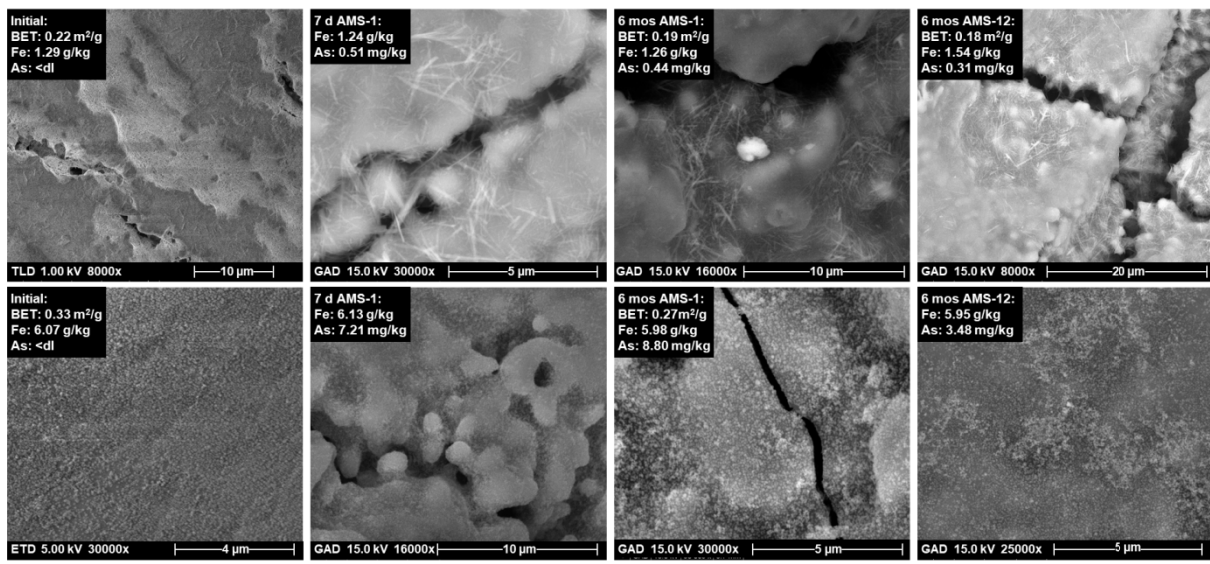
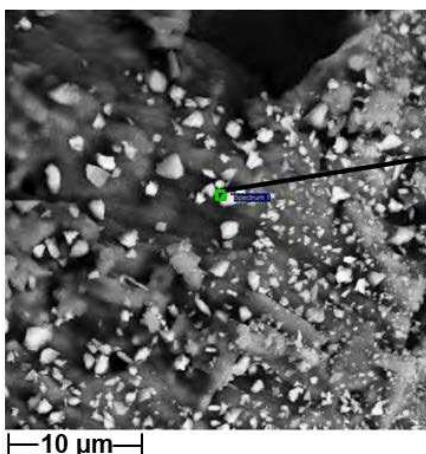


Fig. S8. SEM images of representative sample surfaces before and after *in situ* exposure. Top row: goethite-coated sand; goethite needles show no alteration except for some newly formed mineral phases (see cubic crystals after six months exposure to well AMS-1). Bottom row: hematite-coated sand, which is densely covered by nano-metre sized hematite crystals.

REM images



EDX spectra regions of interest

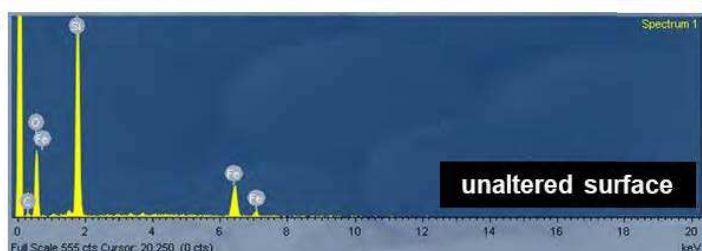
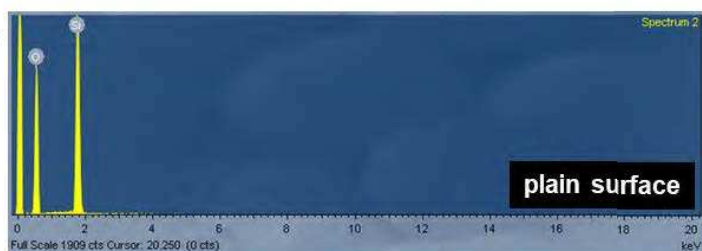
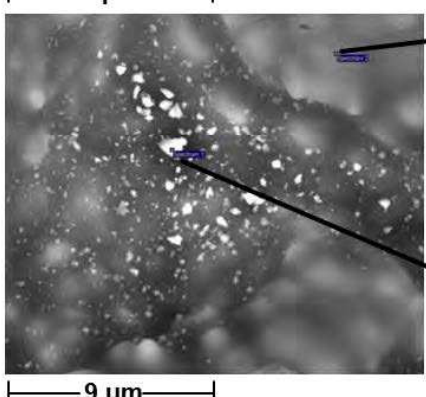
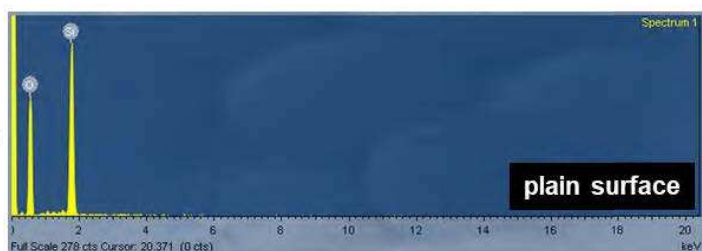
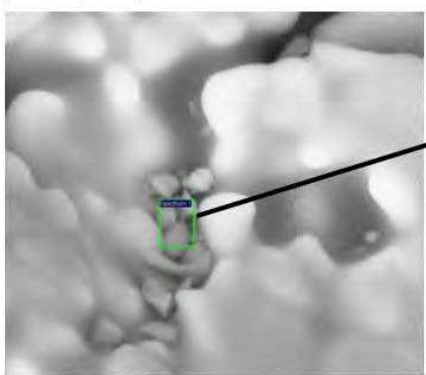
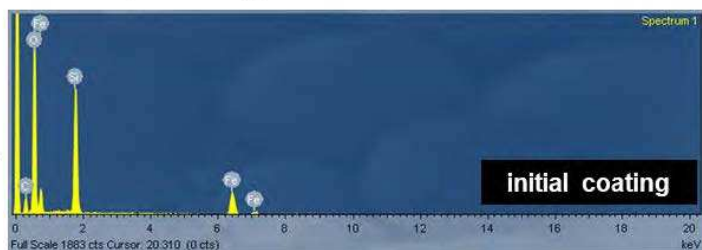
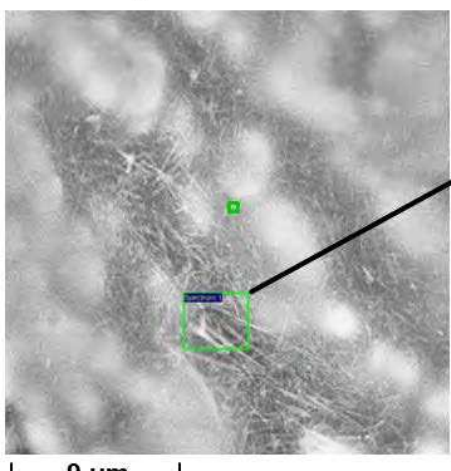


Fig. S9. SEM images of ferrihydrite-coated sand surfaces, including on-spot EDX spectra of selected regions of interest (green squares). Top: surface of the initial ferrihydrite-coated sand covered by sub-micrometer ferrihydrite crystals. Mid: blank surface after long-term (six months) exposure in a highly reducing environment (well AMS-1). Bottom: surface of a ferrihydrite-coated grain after short-term (one week) exposure to a highly reducing groundwater environment (well AMS-1). The coating has partially vanished, leaving large surface areas plain, which is further supported by EDX spectra of two contrasting spots (spectrum 1 focussed on an intact coating, spectrum 2 focused on a plain surface area).

REM images



EDX spectra regions of interest

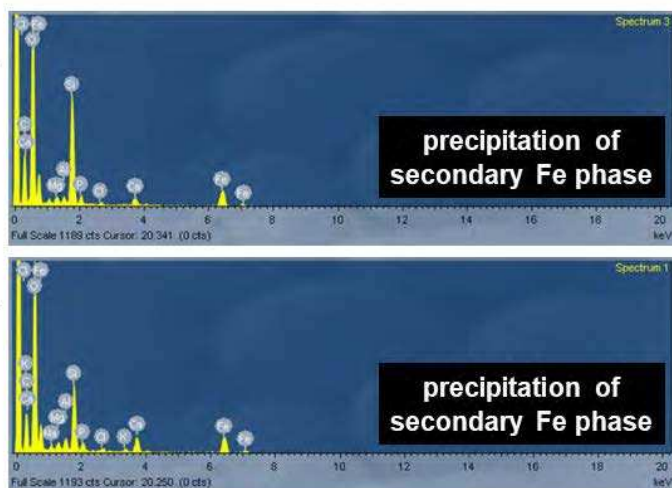
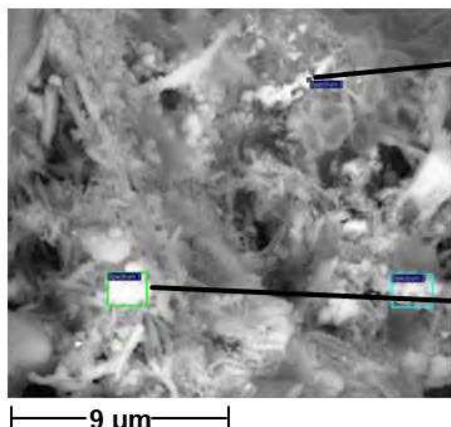
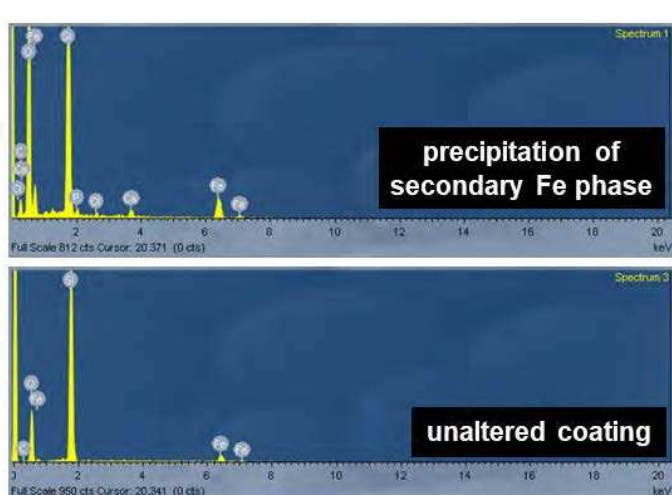
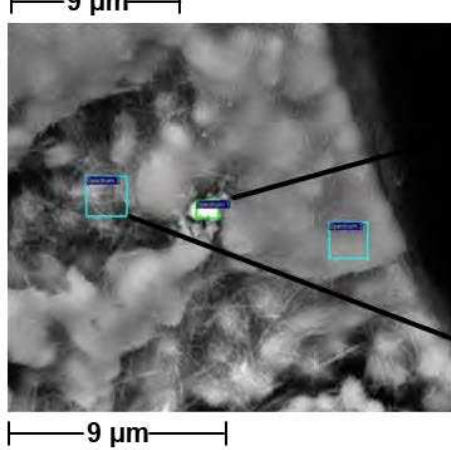
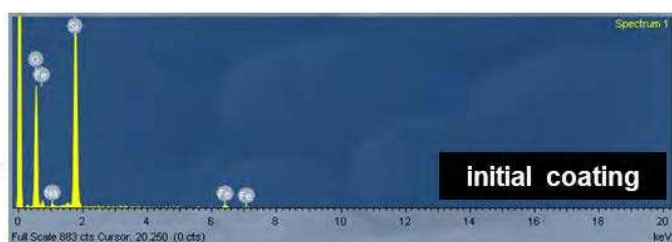
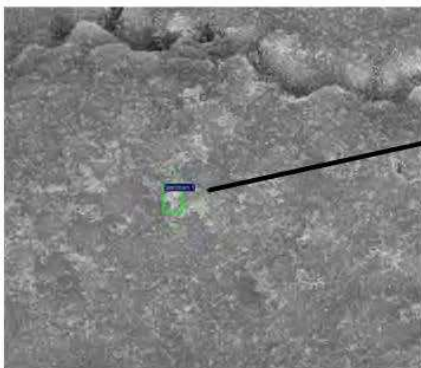


Fig. S10. SEM images and EDX spectra of goethite-coated sand. Top: initial coating of sub-micrometer goethite needles. Mid: after long-term (six months) exposure to reducing groundwater of well AMS-1 (E_h of +45 mV), a punctual formation of cubic Fe minerals occurred, including traces of P and Ca (see respective EDX spectrum 1). Bottom: similar alterations after short-term exposure (one week) to groundwater in this well (AMS-1). EDX spectra reveal newly formed cubic mineral aggregates that contain traces of P, Ca, Mg, K, Al, Na and Cl in addition to Fe and O. The round shaded structures further indicate microbial colonization.

REM images



EDX spectra for regions of interest

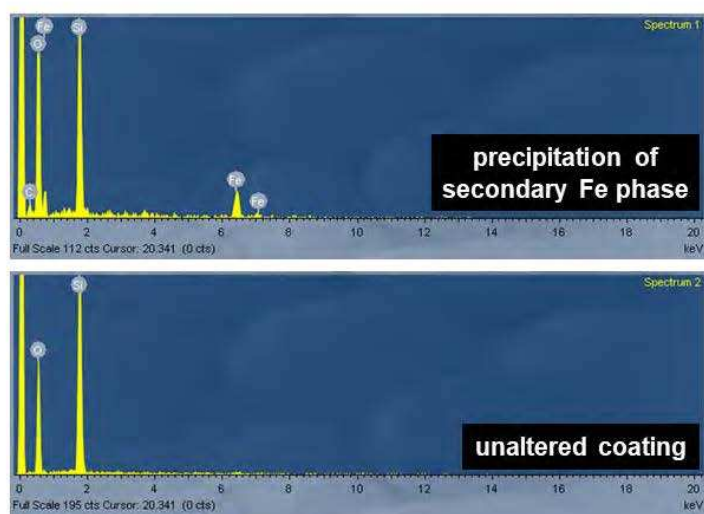
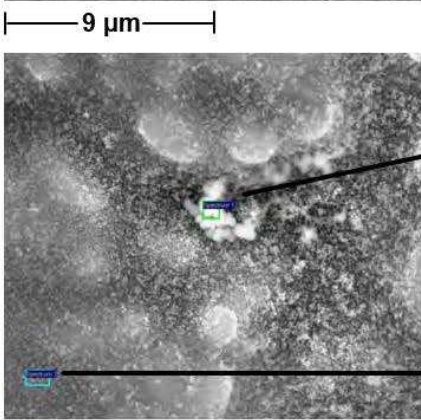
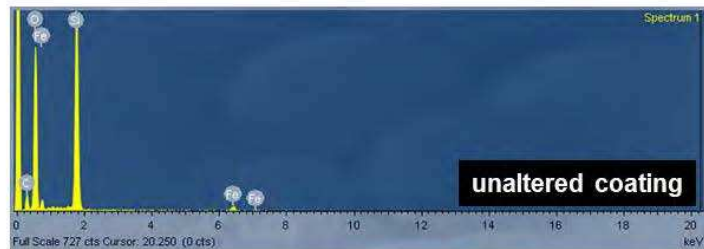


Fig. S11. SEM images and EDX spectra of hematite-coated sand. Top: no change in the surface structure was visible after short-term exposure of one week in a strongly reducing environment (well AMS-5). Bottom: after six months of exposure to strongly reducing groundwater of well AMS-1 a punctual formation of cubic Fe minerals occurred (spectrum 1). These Fe minerals are similar to those observed on the surfaces of the goethite-coated sand (see Fig. S10). In addition, the spiral-shaped structure right next to the newly formed minerals indicates organic matter, which could be related to microbial colonization.

Table S1. Summary of field parameters and water chemistry for groundwater from the experimental wells. The As concentrations in groundwater wells generally remained stable during the 12-months study period (April 2013 to April 2014). The only exception is AMS-5 that showed a permanent increase in As concentrations along with Fe and P between April and October 2013.

well	sampling date	T	EC	pH	E _h	O ₂	DOC	HCO ₃ ⁻	Na	K	Ca	Mg	Si	Cl ⁻	SO ₄ ²⁻	NO ₃ ⁻	NH ₄ ⁺	Fe	Mn	P	As _{tot}	As _{III}	ion balance
		°C	μS/cm	mV	mg/L	mg C/L	mg/L	mmol/L	mmol/L	mmol/L	mmol/L	mmol/L	mmol/L	mmol/L	mmol/L	mmol/L	umol/L	umol/L	umol/L	umol/L	%ratio	% error	
AMS-2*	04/16/2014	25.8	857	7.0	+156	error	1.52	535	0.41	0.23	0.95	2.05	0.34	0.54	0.003	<0.02	2.23	2.09	7.06	1.05	0.003	73.2	-2.34
AMS-4*	04/15/2014	26.0	895	7.0	+159	error	1.21	618	0.57	0.16	1.87	1.69	0.39	0.15	<0.002	<0.02	1.45	2.21	20.7	3.18	0.007	67.0	-4.85
AMS-5	04/15/2014	25.8	1244	6.8	+37	error	13.9	889	0.43	0.19	2.19	1.19	0.55	0.13	0.004	<0.02	5.06	236	2.94	54.6	6.30	99.4	-6.81
AMS-11**	04/16/2014	25.9	909	7.0	+7	error	3.58	643	0.56	0.13	2.33	1.18	0.36	0.17	0.002	<0.02	1.48	193	3.58	22.5	5.35	100	-5.77
AMS-12	04/23/2014	26.6	907	7.0	+11	0.02	1.93	628	0.25	0.07	3.19	1.28	0.50	0.08	<0.05	<0.02	0.03	208	15.0	33.0	2.27	95.7	-3.50
AMS-15	04/16/2014	25.6	517	6.9	+112	0.00	1.56	336	0.54	0.15	0.49	1.06	0.32	0.60	0.008	<0.02	1.26	18.0	21.5	2.29	0.26	97.4	-8.77
AMS-32**	04/15/2014	25.9	881	7.1	-4	error	2.55	592	0.49	0.14	2.33	0.90	0.27	0.15	0.001	<0.02	1.68	147	64.7	25.2	1.87	97.0	-3.67
VPNS-5	04/15/2014	25.9	941	7.0	+23	error	3.00	645	0.54	0.07	2.81	1.27	0.42	0.55	0.002	<0.02	0.61	239	2.45	22.4	5.18	93.6	-6.18
AMS-1**	10/29/2013	25.9	980	7.2	+23	0.13	11.9	616	0.41	0.19	1.78	1.17	0.51	0.25	<0.002	<0.02	3.70	179	4.70	27.1	6.701	92.4	+1.01
AMS-2*	10/24/2013	24.1	842	7.1	+151	0.11	2.14	531	0.44	0.25	0.95	2.19	0.37	0.50	<0.002	<0.02	2.20	0.99	7.22	0.74	<0.001	-	-0.02
AMS-5	10/25/2013	26.1	1273	6.7	+29	0.16	12.8	842	0.46	0.22	2.26	1.29	0.59	0.09	0.004	<0.02	5.23	265	3.26	62.5	6.50	93.3	-1.44
AMS-11**	10/30/2013	26.3	915	7.3	+17	0.13	4.62	618	0.59	0.15	2.41	1.26	0.39	0.24	<0.002	<0.02	nd	202	4.05	24.9	5.27	93.3	-10.6*
AMS-12	10/28/2013	26.6	950	7.3	+9	0.13	2.63	669	0.27	0.07	3.54	1.49	0.54	0.11	0.339	<0.02	0.06	238	17.7	31.8	2.23	92.2	-3.60
AMS-15	10/28/2013	25.7	459	7.1	+118	0.18	3.06	291	0.61	0.17	0.47	1.15	0.35	0.50	0.016	<0.02	0.88	20.6	22.9	1.61	0.26	104	-2.68
AMS-32**	10/24/2013	25.6	889	7.3	-5	0.15	2.81	590	0.55	0.16	2.47	0.99	0.30	0.12	<0.002	<0.02	1.74	156	73.5	28.7	1.85	95.3	+0.12
VPNS-5	10/25/2013	25.9	934	7.3	+3	0.08	4.45	602	0.57	0.08	2.83	1.34	0.45	0.52	<0.002	<0.02	0.73	249	2.65	24.4	5.07	96.5	-0.95
AMS-1**	10/23/2013	26.2	1196	6.7	+45	0.56	10.4	815	0.47	0.20	2.57	1.62	0.52	0.11	0.004	<0.02	3.56	247	8.35	19.0	6.63	104	-1.30
AMS-2*	04/25/2013	26.0	856	6.9	+154	0.37	3.33	525	0.44	0.26	0.93	1.88	0.37	0.40	0.002	<0.02	2.28	3.42	7.68	1.32	0.06	76.2	-2.20
AMS-5	04/25/2013	25.9	1267	6.8	+29	0.36	-	827	0.49	0.21	2.57	1.28	0.57	0.11	0.117	<0.02	4.22	158	11.0	32.2	4.49	error	-3.72
AMS-12	04/25/2013	26.8	883	6.5	+19	0.56	2.05	659	0.25	0.07	3.20	1.29	0.52	0.10	0.009	<0.02	0.06	225	16.9	29.2	2.32	100	-5.34

*Pleistocene aquifer, low As concentrations in groundwater; **Pleistocene aquifer, transition zone, high As concentrations

Table S2. Summary of initial sample materials used for the *in situ* experiments. Total As and Fe concentrations were determined from acid microwave digestions.

sample	grain size (mm)	Fe ($\mu\text{mol/kg}$)	As (nmol/kg)	BET (m^2/g)
cristobalite, uncoated	0.2 - 0.4	<0.32	<0.83	0.105 ± 0.012
two-line ferrihydrite, coated	0.2 - 0.4	15.2 ± 0.2	<0.83	0.348 ± 0.021
hematite-coated sand	0.2 - 0.4	109 ± 2	<0.83	0.331 ± 0.035
goethite-coated sand	0.2 - 0.4	23.2 ± 0.5	<0.83	0.224 ± 0.003
Pleistocene sediment	0.2 - 0.5	45.5 ± 7.3	$6.24 \pm 0.92^*$	0.552
Pleistocene sediment	initial	185 ± 3	19.2 ± 2.9	3.52 ± 0.18

*sequential extraction revealed that As is not surface adsorbed, but incorporated into iron mineral phases

Table S3. Summary of experimental data showing the total Fe and As contents of the samples before and after the *in situ* experiments. The Fe and As contents were determined by ICP-MS from microwave-assisted acid digestion of freeze-dried sample material (note: the sample material was not ground prior to the acid digestion, because only surface sorbed As was targeted). Abbreviations: ferrihydrite-coated sand (Fh), goethite-coated sand (Goe), hematite-coated sand (He), Pleistocene sediments (Ps), methodical detection limit (mdl). Samples analyzed as duplicates (*), triplicates (**), single values (***) due to analytical errors. Note: Pleistocene sediment samples include an initial As content of 0.47 µg/g, which is still included in the values stated below. To calculate the net amount of As sorbed after the *in situ* exposures, this initial amount was later subtracted from the measured sample values.

sampling date	well ID	mineral	exp. time	Fe				As						
				µg/g	±	µmol/g	±	µg/g	±	nmol/kg	±			
mdl (for 50mg sample weight):				17.7		0.32		0.06		0.83				
adsorption experiments:														
ferrihydrite		Fh	initial	851	13	15.2	0.2	<0.06		<0.83				
Apr 14	AMS-5*	Fh	1d	1190	345	21.3	6.2	2.54	0.02	33.8	0.2			
Apr 14	AMS-4*	Fh	7d	828	161	14.8	2.9	<0.06		<0.83				
Apr 14	AMS-11*	Fh	7d	1054	319	18.9	5.7	3.80	0.13	50.8	1.8			
Apr 13	AMS-12*	Fh	7d	589	117	10.5	2.1	1.97	0.10	26.2	1.3			
Apr 14	AMS-15*	Fh	7d	816	246	14.6	4.4	0.67	0.05	8.94	0.68			
Apr 14	AMS-32*	Fh	7d	1170	13	21.0	0.2	1.83	0.12	24.4	1.6			
Apr 13	AMS-5**	Fh	7d	578	23	10.4	0.4	3.52	0.23	47.0	3.1			
Apr 13	AMS-1**	Fh	7d	632	2	11.3	0.0	5.24	0.15	69.9	2.1			
Apr 14	AMS-5*	Fh	8d	909	20	16.3	0.4	4.32	0.13	57.6	1.7			
Oct 13	AMS-1*	Fh	4wks	32.9	11.3	0.59	0.20	0.45	0.01	5.97	0.15			
Oct 13	AMS-15*	Fh	4wks	74.5	8.2	1.33	0.15	0.15	0.02	2.02	0.25			
Oct 13	AMS-32*	Fh	4wks	162	3	2.91	0.05	0.69	0.02	9.21	0.31			
Oct 13	AMS-5*	Fh	4wks	292	7	5.22	0.12	2.61	0.09	34.8	1.2			
Oct 13	VPNS-5*	Fh	4wks	539	579	9.64	10.4	2.15	1.08	28.7	14.4			
Oct 13	AMS-1**	Fh	6mos	<17.7		<0.32		0.31	0.03	4.08	0.41			
Apr 14	AMS-11*	Fh	6mos	104	73	1.9	1.3	1.10	0.88	14.7	11.8			
Oct 13	AMS-12**	Fh	6mos	53.5	1.1	1.0	0.0	0.25	0.01	3.31	0.19			
Apr 14	AMS-12**	Fh	6mos	385	196	6.9	3.5	2.23	0.27	29.7	3.7			
Apr 14	AMS-15*	Fh	6mos	63.7	22.3	1.1	0.4	0.11	0.01	1.48	0.08			
Oct 13	AMS-5**	Fh	6mos	317	145	5.7	2.6	2.92	1.70	39.0	22.7			
Apr 14	AMS-5**	Fh	6mos	281	61	5.0	1.1	2.37	0.41	31.6	5.5			
Apr 14	VPNS-5**	Fh	6mos	230	93	4.1	1.7	2.09	1.68	27.8	22.4			
goethite		Goe	Initial	1300	30	23.2	0.5	<0.06		<0.83				
Apr 14	AMS-5*	Goe	1d	1270	23	22.8	0.4	0.80	0.03	10.7	0.4			
Apr 14	AMS-4*	Goe	7d	1260	1	22.6	0.0	<0.06		<0.83				
Apr 14	AMS-11*	Goe	7d	1300	4	23.3	0.1	0.62	0.03	8.31	0.46			
Apr 13	AMS-12**	Goe	7d	1220	9	21.8	0.2	0.18	0.01	2.44	0.17			

Apr 14	AMS-15*	Goe	7d	1180	24	21.2	0.4	0.09	0.00	1.20	0.03
Apr 14	AMS-32*	Goe	7d	1265	4	22.7	0.1	0.26	0.01	3.45	0.12
Apr 13	AMS-5**	Goe	7d	1441	166	25.8	3.0	0.41	0.05	5.42	0.72
Apr 13	AMS-1**	Goe	7d	1230	6	22.0	0.1	0.51	0.02	6.77	0.23
Apr 14	AMS-5*	Goe	8d	1260	9	22.5	0.2	0.64	0.04	8.49	0.57
Oct 13	AMS-1*	Goe	4wks	1230	25	22.0	0.4	0.50	0.01	6.71	0.08
Oct 13	AMS-15*	Goe	4wks	1190	40	21.3	0.7	<0.06		<0.83	
Oct 13	AMS-32*	Goe	4wks	1260	5	22.6	0.1	0.22	0.01	2.87	0.09
Oct 13	AMS-5*	Goe	4wks	1270	1	22.8	0.0	0.43	0.02	5.69	0.21
Oct 13	VPNS-5*	Goe	4wks	1220	16	21.8	0.3	0.49	0.01	6.53	0.15
Oct 13	AMS-1**	Goe	6mos	1250	22	22.3	0.4	0.43	0.00	5.69	0.04
Apr 14	AMS-11*	Goe	6mos	1220	22	21.9	0.4	0.40	0.05	5.37	0.64
Oct 13	AMS-12**	Goe	6mos	1540	249	27.6	4.5	0.31	0.06	4.15	0.75
Apr 14	AMS-12**	Goe	6mos	1270	66	22.8	1.2	0.24	0.04	3.22	0.56
Apr 14	AMS-15*	Goe	6mos	1190	24	21.2	0.4	<0.06		<0.83	
Oct 13	AMS-5**	Goe	6mos	1280	22	22.9	0.4	0.42	0.02	5.60	0.26
Apr 14	AMS-5**	Goe	6mos	1310	7	23.5	0.1	0.48	0.01	6.37	0.16
Apr 14	VPNS-5**	Goe	6mos	1230	24	22.0	0.4	0.46	0.05	6.17	0.68
hematite		He	Initial	6080	107	109	2	<0.06		<0.83	
Apr 14	AMS-5*	He	1d	5700	95	102	2	3.29	0.01	43.9	0.2
Apr 14	AMS-4*	He	7d	6050	100	108	2	<0.06		<0.83	
Apr 14	AMS-15*	He	7d	5820	173	104	3	1.11	0.04	14.8	0.6
Apr 14	AMS-11*	He	7d	6670	1020	119	18	5.83	0.65	77.8	8.6
Apr 13	AMS-12**	He	7d	5830	40	104	1	2.88	0.06	38.5	0.8
Apr 14	AMS-32*	He	7d	6050	50	108	1	2.92	0.10	38.9	1.4
Apr 13	AMS-5**	He	7d	5650	27	101	0	4.18	0.07	55.8	0.9
Apr 13	AMS-1**	He	7d	6130	820	110	15	7.21	0.73	96.2	9.7
Apr 14	AMS-5*	He	8d	6080	17	109	0	4.12	0.09	55.0	1.2
Oct 13	AMS-1*	He	4wks	5940	395	106	7	8.17	0.53	109	7
Oct 13	AMS-15*	He	4wks	5490	11	98.3	0.2	1.95	0.02	26.0	0.2
Oct 13	AMS-32*	He	4wks	5920	262	106	5	2.69	0.18	35.8	2.5
Oct 13	AMS-5*	He	4wks	6080	217	109	4	5.70	0.17	76.1	2.3
Oct 13	VPNS-5*	He	4wks	5930	91	106	2	6.34	0.11	84.6	1.5
Oct 13	AMS-1**	He	6wks	5980	190	107	3	8.79	0.18	117	2
Apr 14	AMS-11*	He	6mos	5640	1	101	0	6.06	0.04	80.9	0.5
Oct 13	AMS-12**	He	6mos	5950	36	107	1	3.48	0.04	46.5	0.5
Apr 14	AMS-12**	He	6mos	5850	115	105	2	2.74	0.03	36.6	0.4
Apr 14	AMS-15**	He	6mos	5470***	-	98.0	-	2.32	0.69	31.0	9.2
Oct 13	AMS-5**	He	6mos	6020	164	108	3	5.76	0.16	76.9	2.2
Apr 14	AMS-5**	He	6mos	6020	188	108	3	5.33	0.05	71.2	0.7
Apr 14	VPNS-5	He	6mos	5700	38	102	1	5.30	0.06	70.7	0.8
Pleistocene sediment		Ps	Initial	2540	408	45.4	7.3	0.47	0.07	6.24	0.92
Apr 14	AMS-5*	Ps	1d	3020	151	54.0	2.7	1.58	0.40	21.2	5.4
Apr 14	AMS-4*	Ps	7d	2970	185	53.2	3.3	0.51	-	6.80	
Apr 14	AMS-11*	Ps	7d	3000	296	53.8	5.3	1.69	0.14	22.57	1.93

Apr 13	AMS-12**	Ps	7d	2490	277	44.5	5.0	0.92	0.13	12.26	1.73
Apr 14	AMS-15*	Ps	7d	3320	117	59.4	2.1	0.68	0.07	9.09	0.87
Apr 14	AMS-32*	Ps	7d	4260	122	76.3	2.2	1.42	0.12	18.93	1.63
Apr 13	AMS-5**	Ps	7d	2280	220	40.8	3.9	1.15	0.19	15.37	2.51
Apr 13	AMS-1**	Ps	7d	2430	276	43.5	4.9	1.52	0.17	20.28	2.26
Apr 14	AMS-5*	Ps	8d	2820	285	50.6	5.1	1.48	0.07	19.82	1.00
Oct 13	AMS-1**	Ps	4wks	2910	534	52.0	9.6	1.60	0.09	21.35	1.18
Oct 13	AMS-15**	Ps	4wks	2970	458	53.2	8.2	0.81	0.05	10.76	0.72
Oct 13	AMS-32**	Ps	4wks	2960	651	53.0	11.7	0.96	0.09	12.84	1.24
Oct 13	AMS-5**	Ps	4wks	3210	190	57.5	3.4	1.92	0.19	25.57	2.47
Oct 13	VPNS-5**	Ps	4wks	3790	92	67.8	1.6	1.82	0.13	24.24	1.70
Oct 13	AMS-1**	Ps	6mos	2600	448	46.5	8.0	1.59	0.12	21.22	1.57
Apr 14	AMS-11*	Ps	6mos	4670	80	83.6	1.4	2.52	0.34	33.67	4.54
Oct 13	AMS-12**	Ps	6mos	2690	308	48.2	5.5	1.04	0.11	13.82	1.43
Apr 14	AMS-12**	Ps	6mos	3940	59	70.5	1.1	1.61	0.19	21.55	2.58
Apr 14	AMS-15***	Ps	6mos	4250	-	76.0	-	1.09	-	14.48	-
Oct 13	AMS-5**	Ps	6mos	2740	874	49.1	15.6	1.43	0.22	19.03	2.93
Apr 14	AMS-5**	Ps	6mos	4380	355	78.3	6.4	2.59	0.13	34.55	1.80
Apr 14	VPNS-5**	Ps	6mos	3980	645	71.3	11.6	1.85	0.05	24.68	0.70

desorption Experiments:

initial samples before loading

-**	Fh	initial	851	13	15.2	0.2	<0.06	<0.83
-**	Goe	initial	1300	30	23.2	0.5	<0.06	<0.83
-**	He	initial	6080	107	109	2	<0.06	<0.83
-**	Ps	initial	2540	408	45.4	7.3	0.47	0.07

after loading with As by on-site flushing:

Apr 13	AMS-12*	Fh	-	1050	126	18.8	2.2	0.86	0.05	11.5	0.6
Apr 13	AMS-12*	Goe	-	1440	11	25.8	0.2	0.65	0.00	8.69	0.04
Apr 13	AMS-12*	He	-	6850	1110	123	20	1.46	0.31	19.5	4.1
Apr 13	AMS-12*	Ps	-	2910	1215	52.1	21.8	0.94	0.04	12.6	0.5

after 6mos in AMS-2, loaded by on-site flushing:

Oct 13	AMS-2**	Fh	6mos	73.3	44.5	1.31	0.80	<0.06	<0.83		
Oct 13	AMS-2**	Goe	6mos	1100	49	19.6	0.9	<0.06	<0.83		
Oct 13	AMS-2**	He	6mos	5710	288	102	5	0.53	0.04	7.12	0.47
Oct 13	AMS-2**	Ps	6mos	2040	677	36.5	12.1	0.44	0.06	5.94	0.77

initial, loaded with As by 6mos exposure to AMS-12:

Oct 13	AMS-12**	Fh	6mos	53.5	1.1	0.96	0.02	0.25	0.01	3.31	0.19
Oct 13	AMS-12**	Goe	6mos	1540	249	27.6	4.5	0.31	0.06	4.15	0.75
Oct 13	AMS-12**	He	6mos	5950	36	107	1	3.48	0.04	46.5	0.5
Oct 13	AMS-12**	Ps	6mos	2690	308	48.2	5.5	1.04	0.11	13.8	1.4

after 6mos in AMS-2, loaded by exposure to AMS-12:

Apr 14	AMS-2*	Fh	6mos	22.2	4.7	0.40	0.08	0.09	0.04	1.17	0.54
Apr 14	AMS-2*	Goe	6mos	1230	18	22.1	0.3	0.13	0.00	1.71	0.03
Apr 14	AMS-2*	He	6mos	5510	95	98.7	1.7	3.37	0.05	45.0	0.7
Apr 14	AMS-2*	Ps	6mos	2120	265	37.9	4.7	0.74	0.11	9.94	1.43

Table S4a. Saturation index (SI) values calculated for relevant Fe mineral phases using PHREEQC (wateQ4 database) based on groundwater samples from April 2014 (Parkhurst and Appelo 1999).

well	FeIII-(oxy)hydroxides		goethite	hematite	magnetite	siderite	pyrolusite	stremelite	vivianite
	Fe ₃ (OH) ₈	Fe(OH) ₃ (amorph)	FeO(OH)	Fe ₂ O ₃	Fe ₃ O ₄	FeCO ₃	MnO ₂	FePO ₄ ·2H ₂ O	Fe ₃ (PO ₄) ₂ ·8H ₂ O
AMS-2	-3.14	-0.32	+5.60	+13.2	+13.4	-0.61	-13.5	-2.01	-6.15
AMS-4	-3.25	-0.35	+5.58	+13.2	+13.4	-0.58	-13.1	-1.55	-5.34
AMS-11	-2.17	-0.82	+5.10	+12.2	+14.4	+1.42	-18.8	-1.27	+2.25
AMS-32	-2.10	-0.83	+5.09	+12.2	+14.5	+1.37	-17.5	-1.37	+2.33
AMS-1*	-3.97	-1.43	+4.50	+11.0	+12.6	+1.10	-19.2	-1.34	+1.56
AMS-5	-3.02	-1.02	+4.90	+11.8	+13.6	+1.33	-18.9	-0.71	+2.40
VPNS-5	-1.66	-0.58	+5.31	+12.6	+14.8	+1.46	-18.7	-1.02	+2.37
AMS-15	-2.59	-0.43	+5.48	+13.0	+14.0	+0.10	-15.0	-1.53	-2.66
AMS-12	-2.49	-0.93	+5.02	+12.1	+14.2	+1.38	-18.2	-1.12	+2.44

*values from Oct and Apr (pH) 2013

Table S4b. Saturation index (SI) values calculated for relevant Fe mineral phases based on groundwater samples from April 2014 assuming a strongly reducing redox environment with an Eh of -200mV.

well	FeII-(oxy)hydroxides		goethite	hematite	magnetite	siderite	pyrolusite	stremelite	vivianite
	Fe ₃ (OH) ₈	Fe(OH) ₃ (amorph)	FeO(OH)	Fe ₂ O ₃	Fe ₃ O ₄	FeCO ₃	MnO ₂	FePO ₄ ·2H ₂ O	Fe ₃ (PO ₄) ₂ ·8H ₂ O
AMS-2	-15.1	-6.31	-0.39	+1.23	+1.47	-0.61	-25.5	-8.00	-6.14
AMS-4	-15.3	-6.38	-0.46	+1.10	+1.29	-0.57	-25.1	-7.59	-5.33
AMS-11	-9.16	-4.32	+1.61	+5.23	+7.44	+1.42	-25.8	-4.77	+2.25
AMS-32	-8.70	-4.13	+1.79	+5.60	+7.90	+1.37	-24.1	-4.67	+2.33
AMS-1*	-11.5	-5.19	+0.73	+3.48	+5.10	+1.10	-26.7	-5.10	+1.56
AMS-5	-11.0	-5.01	+0.91	+3.84	+5.59	+1.33	-26.8	-4.70	+2.40
VPNS-5	-9.17	-4.34	+1.55	+5.12	+7.32	+1.46	-26.2	-4.78	+2.37
AMS-15	-13.1	-5.68	+0.23	+2.48	+3.47	+0.10	-25.5	-6.78	-2.66
AMS-12	-9.58	-4.47	+1.47	+4.96	+7.10	+1.38	-25.3	-4.67	+2.44

*values from Oct and Apr (pH) 2013

Table S5. Absolute and relative differences between As adsorbed to the Pleistocene sediment after one week and six months. Groundwater As concentrations were measured either directly before or after retrieval of the samples and samples for the one week exposure were either inserted before or after the six month samples, see comments. The amount of As sorbed to the Pleistocene sediment was determined by subtraction of the initial As content (see Table SI 3).

well	1 week ($\mu\text{mol/g}$)	6 months ($\mu\text{mol/g}$)	% increase	groundwater As concentration
AMS-1	14.1 \pm 1.6	15.0 \pm 1.1	+6	1 week: Apr.2013, 6.63 $\mu\text{mol/L}$ 6 months: Apr - Oct 2013, 6.63 / 6.70 $\mu\text{mol/L}$
AMS-5 a	9.13 \pm 1.49	12.8 \pm 2.0	+40	1 week: Apr.2013, 4.49 $\mu\text{mol/L}$ 6 months: Apr - Oct 2013, 4.49 / 6.50 $\mu\text{mol/L}$
AMS-5 b	13.6 \pm 0.7	28.3 \pm 0.5	+108	1 week: Apr.2014, 6.30 $\mu\text{mol/L}$ 6 months: Oct 2013 – Apr 2014, 4.49 / 6.50 $\mu\text{mol/L}$
AMS-11	16.3 \pm 1.40	27.4 \pm 3.7	+68	1 week: Apr.2014, 5.35 $\mu\text{mol/L}$ 6 months: Oct 2013 – Apr 2014, 5.27 / 5.35 $\mu\text{mol/L}$
AMS-12	6.02 \pm 0.85	7.58 \pm 0.78	+26	1 week: Apr.2013, 2.32 $\mu\text{mol/L}$ 6 months: Apr - Oct 2013, 2.32 / 2.23 $\mu\text{mol/L}$
AMS-15	2.86 \pm 0.28	8.25	+189	1 week: Apr.2014, 0.26 $\mu\text{mol/L}$ 6 months: Oct 2013 – Apr 2014, 0.26 / 0.26 $\mu\text{mol/L}$

Supplementary Information Literature:

- Al Lawati, W.M., Rizoulis, A., Eiche, E., Boothman, C., Polya, D.A., Lloyd, J.R., Berg, M., Vasquez-Aguilar, P., van Dongen, B.E., 2012. Characterisation of organic matter and microbial communities in contrasting arsenic-rich Holocene and arsenic-poor Pleistocene aquifers, Red River Delta, Vietnam. *Applied Geochemistry* 27(1), 315-325.
- Eiche, E., 2009. Arsenic Mobilization Processes in the Red River Delta, Vietnam: Towards a Better Understanding of the Patchy Distribution of Dissolved Arsenic in Alluvial Deposits, KIT Scientific Publishing.
- Eiche, E., Neumann, T., Berg, M., Weinman, B., van Geen, A., Norra, S., Berner, Z., Trang, P.T.K., Viet, P.H., Stüben, D., 2008. Geochemical processes underlying a sharp contrast in groundwater arsenic concentrations in a village on the Red River delta, Vietnam. *Applied Geochemistry* 23(11), 3143-3154.
- Guo, H., Zhang, B., Zhang, Y., 2011. Control of organic and iron colloids on arsenic partition and transport in high arsenic groundwaters in the Hetao basin, Inner Mongolia. *Applied Geochemistry* 26(3), 360-370.
- Parkhurst, D.L., Appelo, C., 1999. User's guide to PHREEQC (Version 2): A computer program for speciation, batch-reaction, one-dimensional transport, and inverse geochemical calculations.
- van Geen, A., Bostick, B.C., Thi Kim Trang, P., Lan, V.M., Mai, N.-N., Manh, P.D., Viet, P.H., Radloff, K., Aziz, Z., Mey, J.L., Stahl, M.O., Harvey, C.F., Oates, P., Weinman, B., Stengel, C., Frei, F., Kipfer, R., Berg, M., 2013. Retardation of arsenic transport through a Pleistocene aquifer. *Nature* 501(7466), 204-207.
- Weinman, B., Goodbred, S., Savage, K., Zheng, Y., Radloff, K., Singhvi, A., Charlet, L., Berg, M., Eiche, E., Cribb, W., 2008. The Co-Evolution of Asian Aquifers and Arsenic: How Understanding Sedimentary History can Help Predict Patterns of Arsenic Heterogeneity. *AGU Fall Meeting Abstracts*, Abstr. H52B-04.